Korean J. Electron Microscopy Special Issue 1, 19~24(2006)

# In-situ HRTEM Studies of Alumina-Aluminum Solid-Liquid Interfaces

Sang Ho Oh[1,2,*], Christina Scheu[1,3] and Manfred Rühle[1]
[1]Max-Planck-Institut für Metallforschung, Heisenbergstr. 3, 70569 Stuttgart, Germany
[2]Materials Evaluation Group, Div. of Chemical Metrology and Materials Evaluation, Korea Research Institute of Standards and Science, Daejeon, 305-340, Korea
[3]Physical Metallurgy & Materials Testing, University of Leoben, Franz-Josef-str. 18, A-8700 Leoben, Austria
(Received April 6, 2005; Accepted March 24, 2006)

## ABSTRACT

The alumina-aluminum solid-liquid interfaces were directly observed at atomic scale by heating the alumina single crystal in high-voltage electron microscope (HVEM) owing to the electron beam damage processes. Atomic ordering in the first several layers of the liquid was clearly resolved adjacent to the alumina surface and its relevance to the single crystal growth was examined with the real-time observations.

**Key words** : Alumina-aluminum, Crystal growth In-situ TEM, Irradiation damage, Solid-liquid interfaces

## INTRODUCTION

Understanding the nature of solid-liquid (S-L) interfaces is very important for many processes of technological interest, such as solidification, epitaxial growth, wetting, liquid phase joining, crystal growth, and lubrication. In recent years, many published works report on interesting structural effects occurring at solid-liquid interfaces (Howe, 1994; Saka et al., 1999; Yu et al., 1999; Donnelly et al., 2002; Howe & Saka, 2004).

A S-L interface might not be atomically abrupt in the structural point of view but a structural correlation between two phases can exist across the interface. It has been claimed that the liquid atoms adjacent a solid wall are under the influence of atomic potential of solid atoms so that the atomic ordering in the first several layers of the liquid (three to five layers) will occur, which has been convinced by calculated atomic density profiles across S-L interfaces (Bonissent & Mutaftschiev, 1977; Oxtoby & Haymet, 1982; Curtin, 1987; Hashibon, 2002). Our knowledge on the atomistic structure of S-L interfaces, however, has been limited due to the inherent difficulties associated with direct experimental measurement, much of the current knowledge of S-L interfacial properties has been derived from atomic-scale simulations. Recently, brilliant synchrotron source has been successfully used for probing the atomic ordering in the momentum (reciprocal) space with carefully designed S-L systems (Huisman et al., 1997). Donnelly et al. (2002), for the first time, reported the direct evidence of interfacial ordering of liquid at the S-L interface by high resolution transmission electron microscopy (HRTEM) with fluid xenon confined in faceted cavities in aluminum (Al). However, the liquid phase in their samples is "embedded" inside the crystalline aluminum so that they were obliged to tilt off the sample from the zone axis of Al to evade lattice fringe overlapping while observing the ordered layers. Applying this imaging technique, although successful for showing discrete layering along the one dimension (along the interface normal), they could not get full three dimen-

* Correspondence should be addressed to Dr. Sang Ho Oh, Materials Evaluation Group, Div. of Chemical Metrology and Materials Evaluation, Korea Research Institute of Standards and Science, Daejeon, 305-340, Korea. E-mail: shoh@hrem.mpi-stuttgart.mpg.de or dreathea@hanmail.net

sional spatial information of the ordered layers and their structural correlation with adjacent solid atoms as well.

We report here the real-time observations of the dynamic $Al_2O_3$-Al S-L interfaces by HRTEM at atomic scale. The interfacial conformation of the liquid Al atoms adjacent to the solid alumina is clearly resolved and the transformation of the ordered layers to solid alumina by the layer-by-layer growth mechanism through ledge migration mechanism is directly demonstrated.

## MATERIALS AND METHODS

In-situ heating HRTEM experiments were performed by using Stuttgart high voltage atomic resolution TEM (JEM-ARM 1250, JEOL) operating at 1.25 MeV, which has a point resolution of 0.12 nm. Equipped with the side-entry pole piece, this microscope enables in-situ heating of the specimens up to 1,000°C by using a hot stage holder and a drift compensating device provides highly stable working conditions at elevated temperatures. In addition, for analytical characterization the HVEM is equipped with a post column electron energy loss spectroscopy (EELS) detector (GIF, Gatan). The TEM specimens were made from single crystalline alumina following the conventional dimpling and Ar ion thinning methods. Some of the results presented here were obtained from the cross-sectional TEM specimens made of single crystalline alumina (0001) plates with Cu thin film on top. The TEM specimens were aligned along the zone axes of either the $[01\bar{1}0]$ or $[2\bar{1}\bar{1}0]$ directions of alumina.

The oxidation state of Al in the damaged specimen was identified through post-mortem analytical TEM investigations with SESAM (LEO) at 200 kV and also with VG HB 501 UX dedicated scanning TEM (STEM) operating at 100 kV and equipped with a cold field emission source and a parallel electron energy-loss spectrometer (Gatan UHV Enfina).

## RESULTS AND DISCUSSION

### 1. Electron beam damage processes of alumina: appearance of liquid Al droplets

Since the threshold energy for ballistic knock-on displacement of Al atom (~180 keV) in alumina is much lower than that for oxygen atom (~400 keV), Al atoms are more preferentially displaced from their atomic sites than oxygen and this preference increases with temperature (Pells & Phillips, 1979). In addition, alumina, as a maximal valence oxide, is sensitive to the interatomic ionization by core-hole Auger decay that induces the creation of positively charged oxygen ions, which are then preferentially desorbed from the surface (Knotek & Feibelman, 1978). All these beam damage processes lead to the occurrence of metallic Al in various forms such as surface faceting, interstitial dislocation loops, precipitates or crystallites, depending on the energy of incident electron beam, oxygen pressure of the column and temperature (Pells & Phillips, 1979; Bursill & Lin, 1987, 1989; Bonevich & Marks, 1991; Tomokiyo & Kuroiwa, 1991). In-situ heating in HVEM further accelerates the damage processes of alumina overall and, furthermore, around the melting point of Al (660°C), leads to the evolution of liquid Al droplets. They begin to evolve preferentially from the thin damaged alumina edges, making a contact with alumina in a hemispherical droplet morphology (Fig. 1). The droplets also appear on the bottom surface of rigid region of alumina specimen.

The chemical composition of the liquid droplets was analyzed by using GIF in the HVEM at a temperature of 800°C. The droplets are composed purely of Al with no oxygen detected. The chemical state of Al in the dama-

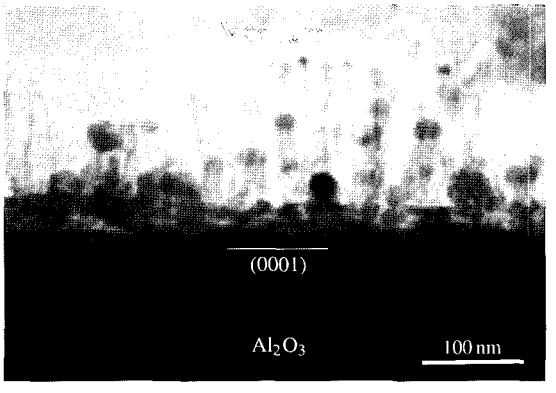


**Fig. 1.** TEM bright field image showing the Al droplets sitting on re-grown alumina whiskers formed by electron beam damage processes. The image was taken in conventional TEM at 854°C.

ged region was further probed in the low energy loss regime of EELS in post-mortem investigations, as the chemical shift is more pronounced in the plasmon loss ($\Delta E \sim 10$ eV) than the core loss of Al. The metallic state Al could successfully mapped out from the oxide state, which is mainly present at the core part of droplets and at thin damaged regions.

## 2. Ordering of liquid Al atoms

Once Al droplets are formed and make a contact with alumina at damaged foil edges, they facilitate a capillary driven re-growth of alumina whiskers, provided that oxygen molecules in the TEM column are transported to the interface plane. The re-grown crystals usually adopt the same orientation of their parent crystal, and thus, the resulting S-L interfaces are parallel in most cases to the orientation of the foil edge (see, e.g. Fig. 1). The S-L interfaces observed in the present study were parallel to the $(2\bar{1}\bar{1}0)$ prism plane (Fig. 2) and to the (0001) basal plane of alumina (Fig. 3). Both the observed S-L interfaces were smooth at atomic scale.

The contrast perturbations observed in the liquid adjacent to the S-L interface (see Fig. 2 and Fig. 3) are attributed to the real structural effect, i. e. the ordering of liquid atoms, as supported molecular dynamic simulation studies as well as the observations of various specimens (orientation) and under different imaging conditions (objective lens defocus). In addition, through the simulation studies to evaluate the effects of imaging artifacts on the ordering contrast in HRTEM, we confirmed that the artifacts alone can not solely account for the experimental contrast perturbations, perhaps they can contribute partly as convoluted to the ordering contrast. The imaging artifacts we studied include: contrast delocalization due to defocus and spherical aberration of the objective lens, Fresnel fringe varying with defocus and a possible tilt of the interface plane along the beam direction.

Figure 2(a) shows the HRTEM image of an Al droplet in contact with re-grown alumina crystal, which was recorded at $\sim 660$°C. The high degree of three dimensional ordering of the liquid Al atoms was clearly resolved near the interface by HRTEM, which persists up to nearly six atomic layers from the interface (Fig. 2 (b) and (c)). The intensity profile acquired with parallel box method shows an exponential decay from the liquid

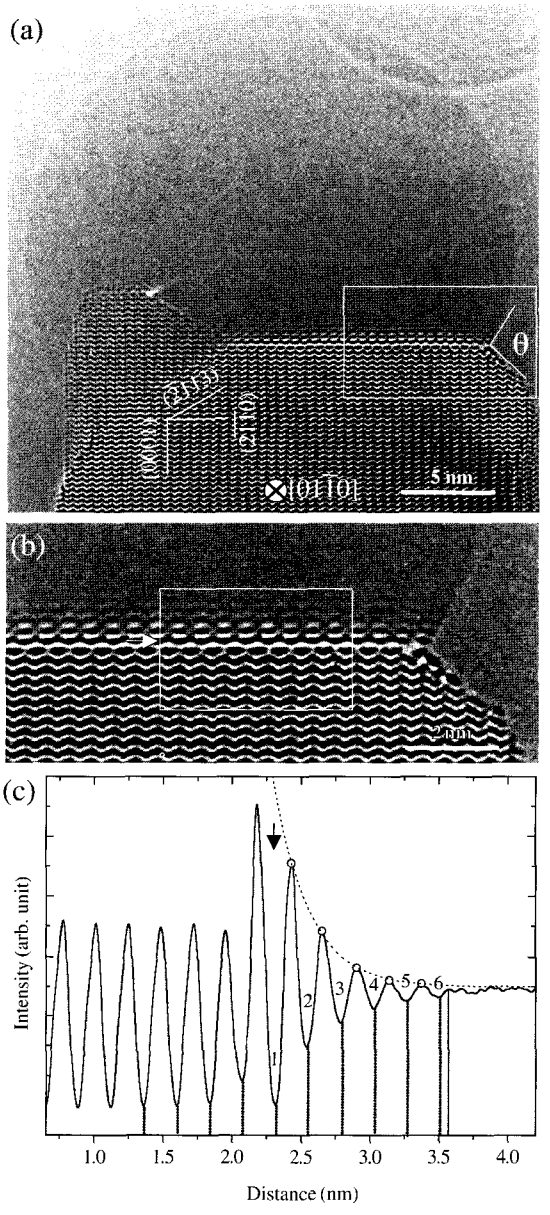


**Fig. 2.** (a) HRTEM image of an aluminum liquid droplet formed on top of an alumina whisker at 654°C. (b) Enlarged view of the white-lined rectangle in (a). (c) Profile intensity of the white-lined rectangle in (b).

side (Fig. 2(c)). The correlation length at the interface, which is inversely proportional to the qualitative measure of disorder, is measured to be $\sim 0.26$ nm by fitting

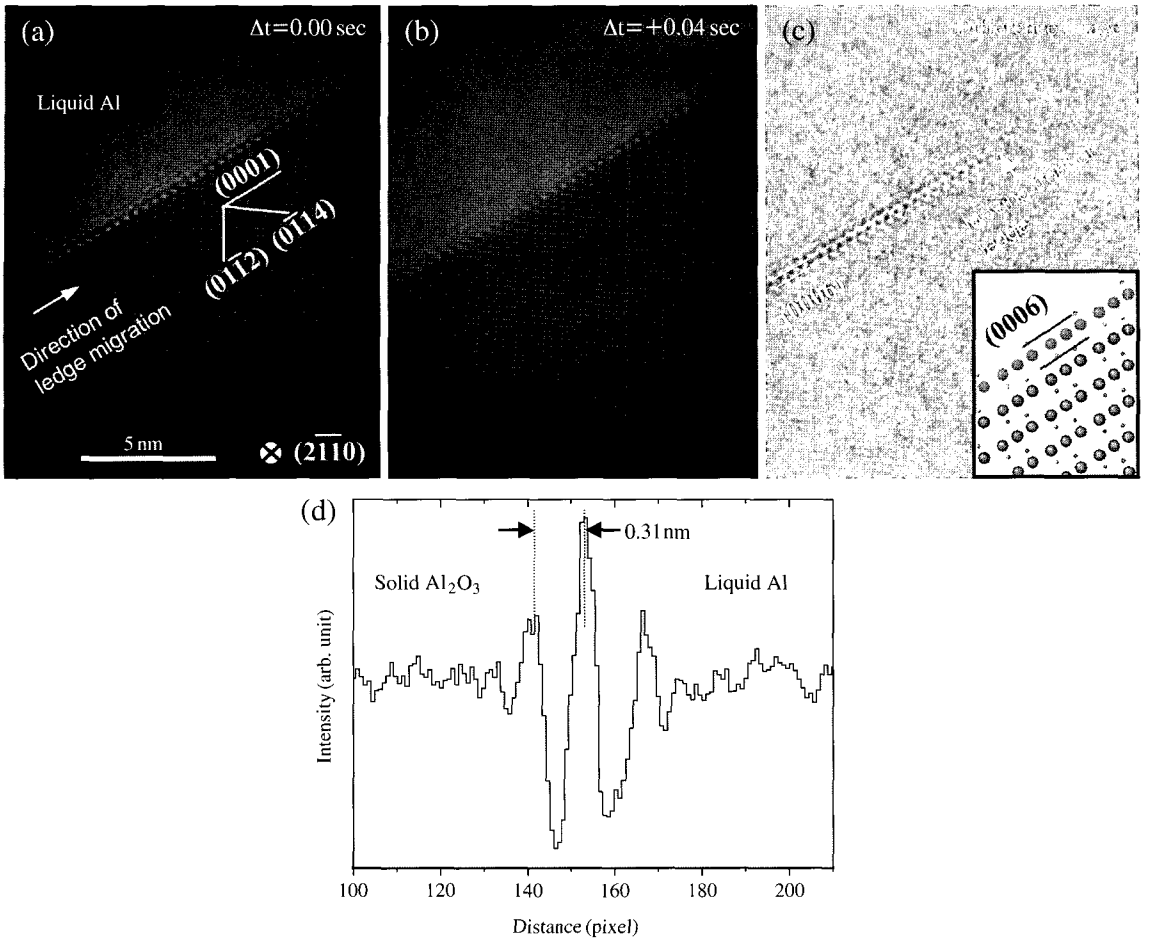


**Fig. 3.** (a), (b) Frame-by-frame HRTEM images of the S-L interface illustrating the ledge migration motion. The frame images were captured from the real-time movie recorded at 854°C in time sequence of 0.04 sec. (c) Difference image obtained by subtracting the image (a) from the image (b). (d) Profile intensity obtained from the difference image of (c) across the interface region.

an exponential function to the intensity maxima. The thin white Fresnel fringe at the crystal and droplet edge indicates that the defocus is around or slightly greater than the Scherzer in thickness-defocus series, assuming that the alumina crystal is no thicker than the width of the Al droplet at its base (~24 nm). At this imaging condition, both the atomic columns of Al and O in alumina exhibit dark contrasts. A simple contrast correlation of the liquid Al to the oxygen sublattice in alumina implies that liquid Al atoms are stacked following hexagonal close packing due to the much stronger Al-O interaction than the Al-Al at the interface, not face centered sequence as in the bulk Al. Since the atomic ordering is a direct result of interaction between liquid Al and solid alumina, the site symmetry in the ordered layer strongly depends on the atomic potential field of solid, which in turn depends on the crystallographic orientation of solid alumina surface, and temperature which determines thermal vibration amplitude of liquid atoms (e.g. compare the different ordering contrast observed in Fig. 3 with Fig. 2). More detailed atomistic simulation is ongoing with effort to find the appropriate atomic potential which well describes the interaction between liquid Al atoms and solid alumina at the interface.

### 3. Dynamic motion of the S-L interface: alumina single crystal growth

The environment of in-situ heating TEM considered (oxygen partial pressure of $10^{-7} \sim 10^{-6}$ Pa, temperature higher than 660°C), solid alumina is the only stable phase of binary Al-O system. The S-L contact system under the irradiation exhibits structural fluctuations intermittently due to the small size effect and at a certain point the capillary driven crystal growth of alumina occurs through the ledge migration mechanism at the S-L interface. The moving ledge unit is observed to be the (0006) plane consisting of two Al and one oxygen layers (Fig. 3(a)-(c)), which was found to nucleate at the triple point. The ledge motion leads to the first ordered layer of liquid aluminum linked to the terminal layer of solid alumina with the aid of oxygen transport, resulting in the formation of Al-O-Al ionic bond (Fig. 3(c)). The velocity of the ledge is estimated to be not less than $4 \times 10^{-5}$ cm/sec at ~850°C within the time resolution of our video system, 0.04 sec. As soon as the first ordered layer incorporates to the alumina crystal by oxygen transport, the atomic rearrangement is accompanied simultaneously in the subsequent ordered layers of liquid Al to re-establish a new equilibrium distribution of liquid atoms; the new equilibrium positions of the ordered layers appear to shift by a half period of ordering, so once the least probable positions for the liquid atoms become the most probable ones. In the difference image of Fig. 3(c), the intensity profile with oscillating and gradually decreasing tail toward the liquid side clearly shows the nature of atomic rearrangement accompanied by the crystal growth.

When the S-L interface energy ($\gamma_{SL}$) was calculated at the triple point by applying Young's equation, it yields ~1.27 J/m$^2$, which is almost same as the surface energy of alumina ($\gamma_{SV}$). The simple liquid droplet on solid wall geometry supposed, it means that the dihedral angle is equivalent to a contact angle of 90°. The contact angle of 90° indicates that the $\gamma_{SV}$ is not lowered by being in contact with the liquid but that the liquid surface energy ($\gamma_{LV}$) is sufficiently lowered by solid for the $\gamma_{SL}$ to become $\gamma_{SV}$. Similar behavior would be expected with any molten metal and its stable lowest valence oxide when the surface energy of the molten metal is greater.

When an Al droplet is in contact with re-grown alumina nano-whisker (Fig. 2), the force balance is achieved at the triple point with the alumina exposing a small ridge and thereby developing a dihedral angle of ~110°. The dihedral angles measured were almost constant in our observations independent of the interface orientation and temperature and they are also very similar to that measured on Sasaki and Saka's HRTEM image. We observed that when the ridge makes a direct contact with liquid Al an oscillatory motion of the ridge, that is crystal growth and dissolution, nucleates a moving ledge and supplies the oxygen atoms required for the continuous growth of the ledge along the interface. For the S-L interface parallel to the (0001) plane (Fig. 3), such a ridge motion was observed to occur with the either of $(01\bar{1}4)$ or $(01\bar{1}2)$ planes.

## SUMMARY

The liquid Al atoms in contact with the alumina surface revealed a high degree of structural correlation to the crystal structure of alumina to even feature a three dimensional ordering. According to the measured dihedral angle at the triple point, the $\gamma_{SL}$ is almost same as the $\gamma_{SV}$ of alumina, which is a direct evidence of such a strong structural correlation at the interface. The layer-by-layer growth of single crystal alumina from liquid Al was observed to proceed by migrating the (0006) ledge, which is nucleated by the oscillatory motion of the small ridge at the triple point. The repetitive growth and dissolution motion of the ridge supply oxygen atoms to the interface and, thus, the rate controlling step of the crystal growth is the interfacial diffusion of oxygen. While the nucleated ledge migrates along the interface in the velocity of $\sim 4 \times 10^{-5}$ cm/sec at ~850°C, the nearby liquid atoms simultaneously adopt a new equilibrium ordered structure.

## ACKNOWLEDGEMENTS

Stimulating discussions with Y. Kauffmann, W. Kaplan and J. Howe are gratefully acknowledged. We are grateful to U. Salzberger and M. Sycha for their excellent TEM specimen preparation, R. Höschen and F. Phillipp for their help at ARM 1250 and W. Siegle for his help during SESAM experiments. This work has

been supported by the German Science Foundation via the Graduiertenkolleg Innere Grenzflächen.

## REFERENCES

Bonevich JE, Marks LD: Ultramicroscopy 35 : 161, 1991.
Bonissent A, Mutaftschiev B: Phil Mag 35 : 65, 1977.
Bursill LA, Lin PJ: Ultramicroscopy 23 : 223, 1987.
Bursill LA, Lin PJ: Phil Mag A 60 : 307, 1989.
Curtin WA: Phys Rev Lett 59 : 1228, 1987.
Donnelly SE, Birtcher RC, Allen CW, Morrison I, Furuya K, Song M, Mitsuishi K, Dahmen U: Science 296 : 507, 2002.
Hashibon A, Alder J, Finnis MW, Kaplan WD: Comp Mater Sci 24 : 443, 2002.
Howe JM: Phil Mag A 74 : 761, 1996.
Howe JM, Saka H: MRS Bulletin 29 : 951, 2004.
Huisman, Peters JF, Zwanenburg MJ, de Vries SA, Derry TE, Abernathy D, van der Veen F: Nature 390 : 379, 1997.
Knotek ML, Feibelman PJ: Phys Rev Lett 40 : 964, 1978.
Oxtoby DW, Haymet ADJ: J Chem Phys 76 : 6262, 1982.
Pells GP, Phillips DC: J Nucl Mater 80 : 207, 1979.
Saka H, Arai S, Tsukimoto S, Sasaki K: Mater Sci Forum 294 : 617, 1999.
Stathopoulos AY, Pells GP: Phil Mag A 47 : 381, 1983.
Tomokiyo Y, Kuroiwa T: Ultramicroscopy 39 : 213, 1991.
Yu CJ, Richter AG, Datta A, Durbin MK, Dutta P: Phys Rev Lett 82 : 2326, 1999.